Local Spectroscopy and Atomic Imaging of Tunneling Current, Forces, and Dissipation on Graphite

S. Hembacher, F. J. Giessibl,* and J. Mannhart
Institute of Physics, Electronic Correlations and Magnetism, Experimentalphysik VI, Universität Augsburg, Universitätsstrasse 1, D-86135 Augsburg, Germany

C. F. Quate
Ginzton Lab, Stanford University, Stanford, California 94305-4085, USA
(Received 27 September 2004; published 9 February 2005)

Theory predicts that the currents in scanning tunneling microscopy (STM) and the attractive forces measured in atomic force microscopy (AFM) are directly related. Atomic images obtained in an attractive AFM mode should therefore be redundant because they should be *similar* to STM. Here, we show that while the distance dependence of current and force is similar for graphite, constant-height AFM and STM images differ substantially depending on the distance and bias voltage. We perform spectroscopy of the tunneling current, the frequency shift, and the damping signal at high-symmetry lattice sites of the graphite (0001) surface. The dissipation signal is about twice as sensitive to distance as the frequency shift, explained by the Prandtl-Tomlinson model of atomic friction.

DOI: 10.1103/PhysRevLett.94.056101 PACS numbers: 68.37.Ef, 62.25.+g, 68.37.Ps, 81.05.Uw

The capability of scanning tunneling microscopy (STM) [1] and atomic force microscopy (AFM) [2] to resolve single atoms in real space makes them powerful tools for surface science and nanoscience. When operating AFM in the repulsive mode, protrusions in the images simply relate to the atoms because of Pauli's exclusion law. In contrast, the interpretation of STM images is more complicated. The Tersoff-Hamann approximation [3], valid for tips in an *s* state, interprets STM images as a map of the charge density of the sample at the Fermi energy. Depending on the state of the tip, atoms can be recorded as either protrusions or holes, and tip changes can reverse the atomic contrast [4,5]. Theoretical predictions regarding the relation of forces and tunneling currents I state that tunneling currents and attractive forces are directly related; thus, AFM would not provide any new physical insights over STM. Chen [5] has found that the square of the attractive energy between tip and sample should be proportional to I with experimental evidence in [6]. Hofer and Fisher [7] suggested that the interaction energy and I should be directly proportional, which is experimentally found in [8,9]. In this Letter, we investigate the experimental relationships between tunneling currents and conservative as well as dissipative forces for graphite probed with a W tip by performing local spectroscopy on *specific* lattice sites. While force spectroscopy on specific lattice sites [10] and combined force and tunneling spectroscopy on unspecific sample positions [8,9] have been performed before, the measurements reported here encompass site-specific spectra of currents *and* forces, supplemented by simultaneous constant-height measurements of currents and forces that allow a precise assessment of the validity of the theories regarding currents and forces in scanning probe experiments.

In graphite (see Fig. 1), the electrons at E_F are concentrated at the β sites, and only these atoms are "seen" by STM at low-bias voltages.

The state-of-the-art method for atomic resolution force microscopy is frequency modulation AFM (FM-AFM) [11], where the frequency shift Δf of an oscillating cantilever with stiffness k, eigenfrequency f_0, and oscillation amplitude A is used as the imaging signal [12,13]. The bonding energy between two adjacent graphite layers at distance σ can be approximated by a Morse potential

$$V_M = E_{\text{bond}}[-2e^{-\kappa(z-\sigma)} + e^{-2\kappa(z-\sigma)}] \qquad (1)$$

with $E_{\text{bond}} \approx -23$ meV and $\kappa \approx 8\ \text{nm}^{-1}$ per atom pair [14]. The "normalized frequency shift" $\gamma(x, y, z) = kA^{3/2}\Delta f(x, y, z)/f_0$ connects the physical observable Δf

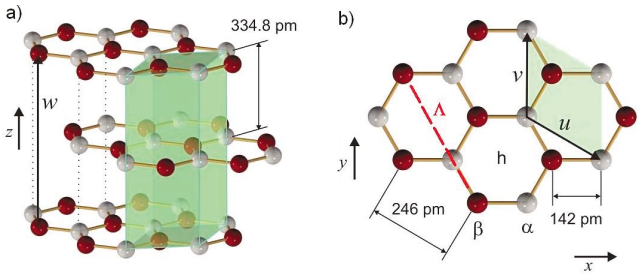

FIG. 1 (color). Crystal structure of graphite. The unit cell (green) consists of two layers with inequivalent basis atoms α (white) and β (red). The α atoms have direct neighbors in the adjacent atomic layers as indicated by the dotted lines; the β atoms are above a hollow site (h). (a) Perspective view, showing three layers formed by hexagonal rings. (b) Top view with surface unit vectors u and v. The line $\Lambda = -v + u$ connects the α, β, and h lattice points, spaced by 142 pm.

and the underlying forces F_{ts} with range λ, where $\gamma \approx 0.4 F_{ts} \lambda^{0.5}$ [see Eqs. (35)–(41) in [13]]. For covalent bonds, the typical bonding strength is on the order of -1 nN with $\lambda \approx 1$ Å, resulting in $\gamma \approx -4$ fN$\sqrt{\text{m}}$, where a negative sign indicates attractive interaction. For graphite, the interlayer bonds are much weaker and the potential of Eq. (1) results in $\gamma_{\text{min}} = -0.1$ fN$\sqrt{\text{m}}$. The interaction of a tip atom with a graphite surface may be stronger than the interlayer bonds but should still result in $-\gamma_{\text{min}} < 1$ fN$\sqrt{\text{m}}$, posing a challenge for AFM imaging. True atomic resolution on graphite by AFM has so far been obtained only at low temperatures, first by Allers *et al.* [15] using large-amplitude FM-AFM with $\Delta f = -63$ Hz, $f_0 = 160$ kHz, $k = 35$ N/m, and $A = 8.8$ nm; thus $\gamma = -11.4$ fN$\sqrt{\text{m}}$. In spectroscopic measurements by the same group, a minimum of $\gamma \approx -60$ fN$\sqrt{\text{m}}$ has been observed [Fig. 1(b) in [16]]. Because this value is more than 2 orders of magnitude greater than the estimate above, it is expected that long-range forces have caused a large contribution in that experiment. Here, we use FM-AFM with sub-nm amplitudes which greatly reduces the influence of long-range forces [13] and enables simultaneous STM operation [17].

We use a low-temperature STM-AFM operating at 4.9 K in ultrahigh vacuum [18]. The microscope uses a qPlus sensor [19] for simultaneous STM-AFM operation ($k = 1800$ N/m, $f_0 = 11\,851.75$ Hz, quality factor $Q = 20\,000$). All data (spectroscopy and images) are recorded at $A = 0.25$ nm. The tip is prepared by dc etching (3 V) of a polycrystalline tungsten wire. The frequency shift is measured with a commercial phase-locked-loop detector (EasyPLL by Nanosurf AG, Liestal, Switzerland). The instrument is thermally well connected to a liquid He bath cryostat at 4.2 K, leading to a drift rate of ≈20 pm/h. Nonconservative tip-sample interactions lead to damping, and the energy ΔE_{ts} that has to be provided for each oscillation cycle to keep A constant is recorded simultaneously with I and Δf.

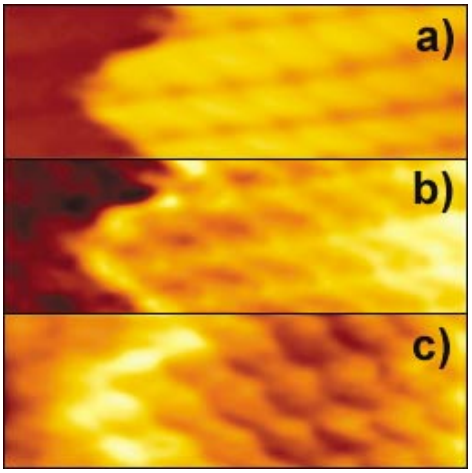

FIG. 2 (color). Simultaneous records of (a) tunneling current, (b) frequency shift, and (c) damping. Image size 3 nm × 1 nm, tip bias 100 mV, and scanning speed 40 nm/s.

To check if the three data channels I, Δf, and ΔE_{ts} are produced by the same tip atom, we have scanned an area that contains a step edge (Fig. 2). The step edge appears at the same position in all three data channels; thus the signals are produced by the same tip atom.

The physics of the interaction is best explored by performing I, γ, and ΔE_{ts} spectroscopy at the high-symmetry lattice sites. Figure 3 shows $I(z)$, $\gamma(z)$, and $\Delta E_{\text{ts}}(z)$ taken at the α-, β-, and h-lattice sites. All three signals initially increase roughly exponentially, as shown in the log-scale insets. The correspondence between experimental images and the lattice sites is established by the analysis below.

The current increases exponentially in the distance regime from $z = 0$ to $z = -100$ pm, followed by a steplike increase for smaller distances. We assume that the tip is essentially in contact with the upper graphite layer for distances smaller than -100 pm. Given that the electrical conductivity of graphite is small at low temperatures and small in the z direction, we conclude that the steplike increase in current for distances smaller than -100 pm is caused by an increasing number of graphite layers becoming available for charge transport. The current spectra in Fig. 3(a) are maximal for most distances on

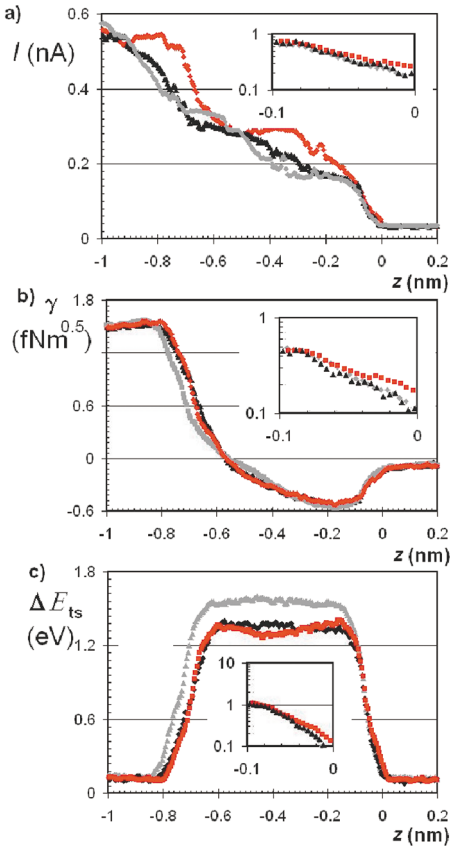

FIG. 3 (color). Experimental spectra of I, γ, and ΔE_{ts} as a function of distance for a tip bias of 160 mV. The gray curves are taken at position "1" in Fig. 4(a), the black curves at position "2," and the red curves at position "3." The insets are views of $I(z)$, $-\gamma(z)$, and $\Delta E_{\text{ts}}(z)$ for -0.1 nm $< z < 0$ on logarithmic scales.

site 3. Because site 3 is a current maximum, we identify it as a β position.

The normalized frequency shift γ decreases down to a distance of ≈ -170 pm, followed by a slight increase down to ≈ -550 pm and a sharper increase for even smaller distances. For $z < -800$ pm, γ remains constant because the cantilever remains in contact with the sample during the entire oscillation cycle. In the z range from 0 to -100 pm where the short-range chemical bonding forces start to emerge, the magnitude of γ increases exponentially (see the inset). It is believed that the short-range forces between AFM tips and graphite originate from van der Waals forces [16] with their typical $1/z^7$-distance dependence. The experimental data shows that when the interatomic distance approaches the atomic diameters, an exponential force dependence prevails.

The damping signal initially also increases exponentially for $z < 0$, reaches a plateau for $z < -170$ pm, decays to zero from $z < -600$ pm, and remains zero for $z < -800$ pm because the cantilever remains in contact for the whole oscillation cycle. This points to a damping mechanism as described by Prandtl [20] and Tomlinson [21], where the energy loss is caused by a plucking action of the atoms on each other. The energy loss per cycle is simply related to the maximal attractive force $F_{ts\,\mathrm{min}}$ and the stiffness of the sample k_{sample} with $\Delta E_{ts} = F_{ts\,\mathrm{min}}^2/(2k_{\mathrm{sample}})$ [22].

The insets are logarithmic plots of $I(z)$, $-\gamma(z)$, and $\Delta E_{\mathrm{ts}}(z)$ for -0.1 nm $< z < 0$, showing an almost exponential distance dependence in that range. For the tunneling current, we find a decay constant $\kappa_I = 13$ nm^{-1} at the β site and $\kappa_I = 15$ nm^{-1} at sites 1 and 2, leading to an apparent barrier height of ≈ 2 eV. The decay constant of γ and thus the interaction potential [Eq. (39) in [13]] is $\kappa_\gamma = 12$ nm^{-1} at the β site and $\kappa_\gamma = 16$ nm^{-1} at sites 1 and 2. The decay constants for κ_I and κ_γ are equal within the measurement accuracy; thus the theory by Hofer and Fisher [7] appears to hold for the interaction of W with graphite. The damping signal decays with $\kappa_{\Delta E_{ts}} = 20$ nm^{-1} at the β site and $\kappa_{\Delta E_{ts}} = 30$ nm^{-1} at sites 1 and 2 as expected from an energy loss proportional to the square of the attractive force.

The normalized frequency spectra shown in Fig. 3(b) are rather similar, except for the gray curve recorded at site 1. In the distance regime from -600 to -800 pm, the gray curve is shifted by ≈ -40 pm. If the C sample atoms and the W tip atom are assumed to be hard spheres with a diameter of 142 and 273 pm, respectively, the W tip atom could protrude 56 pm deeper on top of the hollow sites than at α or β sites. We therefore conclude that position 1 (gray curves) corresponds to a hollow site [h in Fig. 1(b)]. Interestingly, Fig. 3(c) shows that the dissipation is significantly larger on the hollow site than on top of α or β sites. The three data channels were acquired simultaneously and the range from $z = -1.7$ nm to 0.6 nm and back to -1.7 nm was ramped within 60 s. The sequence of the three sites was scanned 3 times, so a total of six spectra was collected for each α, β, and h site. While the drift rate of our instrument is very low, piezocreep caused z offsets of consecutive scans. These offsets were calibrated by comparison with constant-height scans which provide precise cross references for I, γ, and ΔE_{ts} at the α, β, and h sites for a given z value.

The local spectra at high-symmetry sites were supplemented by constant-height scans at various z positions shown in Fig. 4. Figures 4(a)–4(c) show I, γ, and ΔE_{ts} at a tip bias of 160 mV in the fully attractive mode at $z \approx -100$ pm (a), in a weakly repulsive regime at $z \approx -350$ pm (b), and a fully repulsive mode at

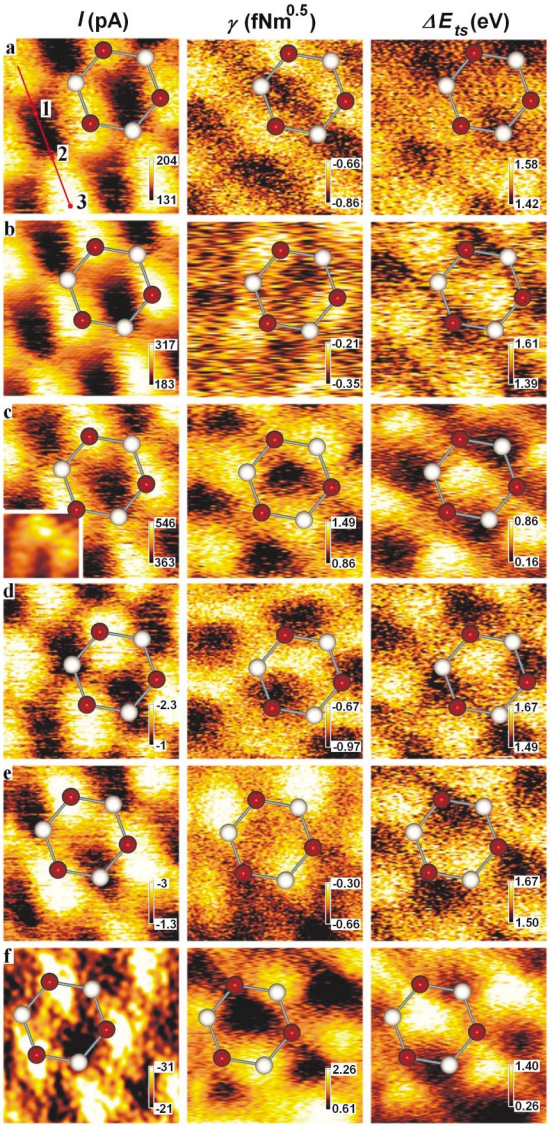

FIG. 4 (color). Constant-height measurements of I, γ, and ΔE_{ts} in attractive and repulsive distance regimes for a tip bias of 160 mV (a)–(c) and -60 mV (d)–(f). The hexagons show the proposed positions of α (white) and β (red) atoms. The brightness is proportional to $|I|$, γ, and ΔE_{ts}. The inset in (c) (left panel) shows a higher harmonic image [23], indicating that the tip state is not perfectly symmetric with respect to the z axis.

$z \approx -750$ pm (c). If the attractive interaction between tip and sample was mediated only by the electronic states that contribute to the tunneling current, the I and γ images in Fig. 4(a) should be exactly inverse. Evidently, this is not the case. We therefore conclude that electronic states that do not contribute to the tunneling current may contribute to attractive interaction. In the repulsive regime shown in Fig. 4(c), the repulsion is strongest above the α sites, almost as strong on the β sites, and weakest on hollow sites, in agreement with Fig. 3(a) and the Pauli exclusion law. The current has a local maximum on top of the β sites, and ΔE_{ts} has a pronounced maximum at the hollow sites. Because of the long time scales involved in damping measurements, atomically resolved energy loss measurements are prone to lateral shifts [24] for fast scanning. The scanning speeds used in the data of Fig. 4 were ≈ 0.3 nm/s; therefore, time delays in the acquisition channels are negligible, and the I, γ, and ΔE_{ts} images match precisely in forward and backward scans. In our previous simultaneous STM-AFM measurement on graphite [17], we found a lateral shift of 68 pm of the current maxima with respect to the corresponding γ maxima. While the tip is not perfectly symmetric with respect to the z axis (see the Fig. 4 caption), it is evidently more symmetric than in [17]. Arai and Tomitori [25] have recently shown that force interactions are also a function of bias. Figures 4(d)–4(f) show constant-height images at a different tip bias of -60 mV. In the attractive regime shown in Fig. 4(d), the I and γ images are approximately inverse; i.e., the local minimum in γ coincides with the local maxima in I. In the repulsive regime shown in Fig. 4(f), again the repulsion is strongest above the α sites, almost as strong on the β sites, and weakest on hollow sites.

While the distance dependencies of current, force, and dissipation as revealed by constant-height images and local spectroscopic measurements are qualitatively similar, the contrast observed in the constant-height images is larger than expected from the local spectra. The reason for these subtle discrepancies is revealed by the constant-height data shown in Fig. 4. Frequency shift and current images are different in all distance regimes, and slight shifts between the high-symmetry points in I and γ images are present.

In summary, the spectroscopy experiments show that the z dependence of force and current is roughly the same as predicted in Hofer-Fisher theory [7] for graphite. However, the constant-height experiments prove that attractive forces and currents are *not* directly related and STM and AFM do provide different information. The dissipation measurements reveal that the theories on atomic friction introduced by Prandtl [20] and Tomlinson [21] are the key mechanism for damping on the atomic scale when imaging soft samples. The spatial resolution that is possible by scanning probe microscopy scales with the decay lengths of physical observables [26]. At the onset of damping, the decay length of dissipation is only half the value of the force. This offers an alternate explanation of the impressive resolution obtained in damping images [27].

This work is supported by the Bundesministerium für Bildung und Forschung (Project No. EKM13N6918). We thank M. Herz for discussions and K. Wiedenmann and H. Bielefeldt for help in the construction of the microscope.

*Electronic address: franz.giessibl@physik.uni-augsburg.de

[1] G. Binnig, H. Rohrer, C. Gerber, and E. Weibel, Phys. Rev. Lett. **49**, 57 (1982).
[2] G. Binnig, C. F. Quate, and C. Gerber, Phys. Rev. Lett. **56**, 930 (1986).
[3] J. Tersoff and D. R. Hamann, Phys. Rev. Lett. **50**, 1998 (1985).
[4] J. V. Barth, H. Brune, G. Ertl, and R. J. Behm, Phys. Rev. B **42**, 9307 (1990).
[5] C. J. Chen, J. Phys. Condens. Matter **3**, 1227 (1991).
[6] C. Loppacher, M. Guggisberg, S. Schär, R. Bennewitz, O. Pfeiffer, M. Bammerlin, V. Barwich, A. Baratoff, E. Meyer, and H.-J. Güntherodt, Phys. Rev. B **62**, 16 944 (2000).
[7] W. A. Hofer and A. J. Fisher, Phys. Rev. Lett. **91**, 036803 (2003).
[8] A. Schirmeisen, G. Cross, A. Stalder, P. Grütter, and U. Dürig, New J. Phys. **2**, 29 (2000).
[9] G. Rubio-Bollinger, P. Joyez, and N. Agrait, Phys. Rev. Lett. **93**, 116803 (2004).
[10] M. Lantz, H. J. Hug, R. Hoffmann, P. van Schendel, P. Kappenberger, S. Martin, A. Baratoff, and H.-J. Güntherodt, Science **291**, 2580 (2001).
[11] T. R. Albrecht, P. Grutter, H. K. Horne, and D. Rugar, J. Appl. Phys. **69**, 668 (1991).
[12] R. Garcia and R. Perez, Surf. Sci. Rep. **47**, 197 (2002).
[13] F. J. Giessibl, Rev. Mod. Phys. **75**, 949 (2003).
[14] M. C. Schabel and J. L. Martens, Phys. Rev. B **46**, 7185 (1992).
[15] W. Allers, A. Schwarz, U. D. Schwarz, and R. Wiesendanger, Appl. Surf. Sci. **140**, 247 (1999).
[16] H. Hölscher, A. Schwarz, W. Allers, U. D. Schwarz, and R. Wiesendanger, Phys. Rev. B **61**, 12 678 (2000).
[17] S. Hembacher, F. J. Giessibl, J. Mannhart, and C. F. Quate, Proc. Natl. Acad. Sci. U.S.A. **100**, 12539 (2003).
[18] S. F. Hembacher, Ph.D. thesis, Universität Augsburg, Augsburg, Germany, 2003.
[19] F. J. Giessibl, Appl. Phys. Lett. **73**, 3956 (1998).
[20] L. Prandtl, Z. Angew. Math. Mech. **8**, 85 (1928).
[21] G. A. Tomlinson, Philos. Mag. **7**, 905 (1929).
[22] F. J. Giessibl, H. Bielefeldt, S. Hembacher, and J. Mannhart, Ann. Phys. (Leipzig) **10**, 887 (2001).
[23] S. Hembacher, F. J. Giessibl, and J. Mannhart, Science **305**, 380 (2004).
[24] M. Gauthier, R. Perez, T. Arai, M. Tomitori, and M. Tsukada, Phys. Rev. Lett. **89**, 146104 (2002).
[25] T. Arai and M. Tomitori, Phys. Rev. Lett. **93**, 256101 (2004).
[26] E. Stoll, Surf. Sci. Lett. **143**, L411 (1984).
[27] H. J. Hug and A. Baratoff, in *Noncontact Atomic Force Microscopy*, edited by S. Morita, R. Wiesendanger, and E. Meyer (Springer, Berlin, Heidelberg, New York, 2002), Chap. 20, pp. 395–432.